ORIGINAL ARTICLE

Potato StMPK7 is a downstream component of StMKK1 and promotes resistance to the oomycete pathogen *Phytophthora infestans*

Houxiao Zhang [1,2] | Fangfang Li [1,2] | Zhenzhen Li[1,2] | Jing Cheng[1,2] | Xiaokang Chen [1,2] | Qinhu Wang [3] | Matthieu H.A.J. Joosten [4] | Weixing Shan [5] | Yu Du [1,2]

[1]College of Horticulture, Northwest A&F University and State Key Laboratory of Crop Stress Biology for Arid Areas, Yangling, China

[2]Shaanxi Engineering Research Center for Vegetables, Yangling, China

[3]State Key Laboratory of Crop Stress Biology for Arid Areas and College of Plant Protection, Northwest A&F University, Yangling, China

[4]Laboratory of Phytopathology, Wageningen University, Wageningen, Netherlands

[5]State Key Laboratory of Crop Stress Biology for Arid Areas and College of Agronomy, Northwest A&F University, Yangling, China

Correspondence
Yu Du, College of Horticulture, Northwest A&F University and State Key Laboratory of Crop Stress Biology for Arid Areas, Yangling, Shaanxi 712100, China.
Email: yu.du@nwafu.edu.cn

Funding information
the Programme of Introducing Talents of Innovative Discipline to Universities (Project 111), Grant/Award Number: no. B18042; the Northwest A&F University Scientific Research Fund for Advanced Talents and the Young Talent Training Program: , Grant/Award Number: 2452018028 and 2452017069; China Postdoctoral Science Foundation, Grant/Award Number: 2016M600818 and 2019T120956; National Natural Science Foundation of China, Grant/Award Number: 31701770 and 32072401

Abstract

A cascade formed by phosphorylation events of mitogen-activated protein kinases (MAPKs) takes part in plant stress responses. However, the roles of these MAPKs in resistance of potato (*Solanum tuberosum*) against *Phytophthora* pathogens is not well studied. Our previous work showed that a *Phytophthora infestans* RXLR effector targets and stabilizes the negative regulator of MAPK kinase 1 of potato (StMKK1). Because in *Arabidopsis thaliana* the AtMPK4 is the downstream phosphorylation target of AtMKK1, we performed a phylogenetic analysis and found that potato StMPK4/6/7 are closely related and are orthologs of AtMPK4/5/11/12. Overexpression of StMPK4/7 enhances plant resistance to *P. infestans* and *P. parasitica*. Yeast two-hybrid analysis revealed that StMPK7 interacts with StMKK1, and StMPK7 is phosphorylated on flg22 treatment and by expressing constitutively active StMKK1 (CA-StMKK1), indicating that StMPK7 is a direct downstream signalling partner of StMKK1. Overexpression of StMPK7 in potato enhances potato resistance to *P. infestans*. Constitutively active StMPK7 (CA-StMPK7; StMPK7$^{D198G, E202A}$) was found to promote immunity to *Phytophthora* pathogens and to trigger host cell death when overexpressed in *Nicotiana benthamiana* leaves. Cell death triggered by CA-StMPK7 is SGT1/RAR1-dependent. Furthermore, cell death triggered by CA-StMPK7 is suppressed on coexpression with the salicylate hydroxylase NahG, and StMPK7 activation promotes salicylic acid (SA)-responsive gene expression. We conclude that potato StMPK7 is a downstream signalling component of the phosphorelay cascade involving StMKK1 and StMPK7 plays a role in immunity to *Phytophthora* pathogens via an SA-dependent signalling pathway.

KEYWORDS

MAPK, oomycete, *Phytophthora infestans*, plant resistance, potato

---

Houxiao Zhang and Fangfang Li contributed equally to this work.

1 | INTRODUCTION

The oomycete plant pathogen *Phytophthora infestans* causes the most notorious disease on potato, known as potato late blight, which under humid and cool conditions can devastate a susceptible crop within 2 weeks (Fry, 2008). Although for many years potato breeders have brought resistance genes from wild potato varieties into cultivated potatoes, potato late blight disease is still the number one problem in potato production, and control of the disease is still largely dependent on fungicide sprays. Potato resistance genes against late blight are all from the nucleotide-binding leucine-rich repeat (NLR) gene family (Du et al., 2015). NLR genes confer race-specific resistance against late blight, and each NLR is proposed to recognize a corresponding RXLR effector of *P. infestans* and triggers effector-triggered immunity (ETI). Consequently, resistance provided by NLR genes is easily broken by *P. infestans* isolates that have lost the corresponding RXLR effector gene (Vleeshouwers et al., 2011). For example, the NLR gene *R1* resistance is broken by *P. infestans* isolates that have deleted *AVR1* in their genome (Du et al., 2015), whereas *R3a* resistance is broken by a point mutation in the gene encoding the AVR3a effector (Engelhardt et al., 2012). Currently, in potato production the loss of resistance of originally resistant cultivars is becoming a serious problem. Plant basal resistance is an important part of microbe-associated molecular pattern (MAMP)-triggered immunity (MTI), which is conferred by plasma membrane-localized receptor-like proteins (RLPs), lacking a cytoplasmic kinase domain, or receptor-like kinases (RLKs) proteins that do have such a domain, together known as pattern recognition receptors (PRRs) (Jones & Dangl, 2006).

Mitogen-activated protein kinase (MAPK) cascades exist widely in eukaryotes, and in plants they participate in responses to biotic and abiotic stresses, hormones, cell differentiation, and developmental processes. On immune activation, MAPK cascades transduce signals through phosphorylation by upstream MAPKKKs/MEKKs to their downstream targets, eventually activating the immune response in the nucleus as a result of transcription factor phosphorylation (Pitzschke, Schikora, et al., 2009). A MAPK cascade normally comprises a MAP kinase kinase kinase (MAPKKK, or MEKK), a downstream MAP kinase kinase (MAPKK), and a further downstream MAP kinase (MPK) (Kong et al., 2012), and the activation of upstream MAPKKKs results in the sequential phosphorylation of downstream MKKs and MPKs. On MTI activation, plants activate at least two different MAPK cascades, which are the MKKK-MKK4/5-MPK3/6 cascade and the MEKK1-MKK1/2-MPK4 cascade (Zhang et al., 2017). Activated MPK3/6 subsequently enhance the expression of defence-related genes, such as the gene encoding the fructokinase FRK1 and the transcription factors WRKY22 and WRKY29, thereby mounting immunity to bacteria and fungi (Asai et al., 2002; Wang et al., 2018). MAPK cascades also participate in ETI. For instance, tomato LeMPK1, LeMPK2, and LeMPK3 all participate in the hypersensitive response triggered upon recognition of the Avr4 effector of the fungal pathogen *Cladosporium fulvum* by the Cf-4 resistance protein of tomato (Stulemeijer et al., 2007), potato MAP3K proteins StMAP3Kε and StMAP3Kβ2 function in plant

immunity to *P. infestans* (King et al., 2014; Ren et al., 2019), whereas rice OsMAPK6 participates in *Pit*-mediated resistance to rice blast disease (Kawano et al., 2010). Furthermore, the MEKK1-MKK1/2-MPK4 cascade in the model plant *Arabidopsis thaliana* is monitored by the NLR protein SUMM2, and perturbation of this cascade activates SUMM2-mediated immunity (Zhang et al., 2012).

The *Arabidopsis* genome encodes 20 MPK proteins and phylogenetic analysis of these MPKs shows that they can be divided into four clades, labelled from A to D (Ichimura et al., 2002). The conserved motif of MPKs, which is phosphorylated by upstream MPKKs, TxY, of which the tyrosine (Y) residue is phosphorylated, can be classified into two subtypes, the TEY and TDY subtypes. The TEY subtype is classified into clades A, B, and C, whereas the TDY subtype forms clade D. The clade B MPKs participate in plant growth and development, and responses to biotic and abiotic stress. For example, rice OsMPK6 negatively regulates resistance to *Xanthomonas oryzae* (Yuan et al., 2007), whereas tomato SlMPK4 positively regulates resistance to *Botrytis cinerea* (Virk et al., 2013) and *Nicotiana attenuata* MPK4 participates in the response to insects (Hettenhausen et al., 2013).

MAPK cascades were also found to participate in plant hormone signalling to modulate immunity to insects and microbial pathogens (Hou et al., 2013; Jagodzik et al., 2018). For example, tomato MPKs are known to regulate jasmonic acid (JA) biosynthesis and thereby JA-related gene expression to modulate immunity against herbivorous insects (Kandoth et al., 2007). *Arabidopsis* MPK3 was found to suppress flg22-induced salicylic acid (SA) accumulation (Frei dit Frey et al., 2014). There are also MPK(K)s that participate in both JA and SA signalling, that is, AtMPK4, AtMPK6, SIMKK4, and SIMKK9 (Chai et al., 2014; Li et al., 2014; Pitzschke, Djamei, et al., 2009).

MAPK cascade proteins have been extensively studied in model plants. However, there are only a few studies described that concern the role of MAPK proteins in immunity in crop plants, for instance potato. The StMEK1-StMPK1/StWIPK (the orthologs of *Arabidopsis* AtMKK4/5-AtMPK6/3) cascade is reported in potato to participate in immunity to *P. infestans* (Yamamizo et al., 2006). Our previous work showed that a *P. infestans* RXLR effector targets and stabilizes the potato negative immune regulator StMKK1 (Du et al., 2021). AtMPK4 is the downstream signalling target of AtMKK1/2 in immunity (Zhang et al., 2012), while AtMPK5 was known to be activated by AtMKK2 under stress conditions (Teige et al., 2004). To investigate the downstream immune signalling target of potato StMKK1, we BLAST-searched the potato genome with the AtMPK4 amino acid sequence and performed a phylogenetic analysis of potato clade B MPKs. We identified three orthologous MPK proteins in potato, and named them StMPK4/6/7 according to their tomato orthologs (Virk et al., 2013), as orthologs of AtMPK4/5/11/12. Inoculation assays showed that StMPK4 and StMPK7 participate in immunity to *Phytophthora* pathogens, while StMPK6 does not show such a role. Silencing of the *NbMPK4/6/7* genes in *N. benthamiana* also showed that *NbMPK7* and *NbMPK4* participate in resistance to *Phytophthora* pathogens. The potato stable overexpression (OE) transformants *StMPK7*-OE lines show enhanced resistance to *P. infestans*. To

determine whether StMPK7 functions as a downstream signalling target of StMKK1 in plant immunity, we confirmed that an interaction takes place between StMPK7 and StMKK1 and observed that StMPK7 is phosphorylated by a constitutively active form of StMKK1 (CA-StMKK1). A constitutively active form of StMPK7 (CA-StMPK7) was found to promote immunity to *P. infestans* and *Phytophthora parasitica* and to trigger cell death when overexpressed in *N. benthamiana* leaves. Taken together, we conclude that potato StMPK7 is a downstream signalling component of StMKK1 and plays a role in immunity to *Phytophthora* pathogens.

2 | RESULTS

2.1 | Identification and phylogenetic analysis of StMPK7

To identify the potato orthologs of MPK4/5, we BLAST-searched the predicted proteomes of potato, tomato, and *N. benthamiana* (sol genomics network, https://solgenomics.net/tools/blast/) with the AtMPK4 protein sequence as a query and identified several homologous proteins. Because AtMPK4 and AtMPK5 are closely related proteins that belong to the clade B MPKs, we performed a phylogenetic analysis of clade B MPKs using the MPK protein sequences of various Solanaceae, *Populus*, *Oryza*,

and *Arabidopsis*. Our phylogenetic tree showed that there are two proteins of potato (StMPK4, PGSC0003DMP400000144 and StMPK6, PGSC0003DMP400037535) that are orthologous proteins of *Arabidopsis* AtMPK4/11/12, whereas StMPK7 (PGSC0003DMP400021542) is the orthologous protein of AtMPK5 (Figure 1). Phylogenetic analysis showed that potato MPK4/6/7 are closely related homologous proteins belonging to subclade B1 of the clade B MPKs. These subclade B1 MPKs contain four MPKs MPK4/5/11/12 from *Arabidopsis*, four from *Populus*, two from *Oryza*, and three MPKs from tomato and potato. It seems that the duplication of solanaceous subclade B1 MPKs occurred twice independently, once in the common ancestor of *Arabidopsis*, *Populus*, and Solanaceae, and once in the common ancestor of solanaceous plants (Figure 1).

2.2 | *StMPK7* and *StMPK4* promote plant resistance to *Phytophthora* pathogens

We cloned all three genes encoding the potato MPK4/6/7 homologs. To study the role of potato StMPK4/6/7 in plant defence to *P. infestans*, green fluorescent protein (GFP)-β-glucuronidase (GUS) and GFP-StMPK7 were transiently expressed in the left and right panels of *N. benthamiana* leaves, respectively, and *P. infestans* was inoculated onto the leaves at 1 day after agroinfiltration. The

FIGURE 1 Phylogenetic analysis of clade B MPK proteins from *Arabidopsis*, *Populus*, various Solanaceae, and *Oryza*. The phylogenetic tree was inferred by the maximum-likelihood method, using PhyML. The SH-like support values of branches that represent the lower or higher values are indicated by dots from blueto red. The homologous proteins were BLAST-searched against the genomes of *Arabidopsis, Populus*, Solanaceae, and *Oryza*

results showed that, when compared to the GFP-GUS-expressing leaf halves, GFP-StMPK7 expression resulted in significantly smaller lesions (Figure 2a–c), indicating that StMPK7 positively regulates resistance to *P. infestans*. To investigate whether StMPK7 has a similar role in resistance to other *Phytophthora* pathogens, *P. parasitica* was also inoculated onto the leaves. The results showed that StMPK7 also promotes resistance to *P. parasitica* (Figure 2d–f). The roles of StMPK4 and StMPK6 in plant immunity were also investigated in a similar way. It was observed that StMPK4 promotes plant resistance to both *P. infestans* and *P. parasitica*, while StMPK6 does not appear to play a role in immunity (Figure S1). The accumulation of the StMPK7/4/6 proteins and the controls GFP-GUS and GUS-myc was confirmed by western blotting, as shown in Figure S1j.

To further investigate the role of MPK4/6/7 in *N. benthamiana* immunity, we silenced *NbMPK7* (Figure 3), *NbMPK4*, and *NbMPK6* (Figure S2) in *N. benthamiana* and inoculated the silenced plants with *P. infestans* or *P. parasitica*. Detached leaf assays revealed that, when compared to the control TRV-*GUS*, the *NbMPK7*- and *NbMPK4*-silenced plants developed larger lesions, while the *NbMPK6*-silenced plants did not show altered immunity to the *P. infestans* (Figures S2 and S3), which confirms the positive roles that *MPK7* and *MPK4* play in plant resistance to *Phytophthora* pathogens. *NbMPK7* and *MPK6* silencing does not alter plant morphology, while *NbMPK4* silencing results in larger plants when compared to the control treatment (Figure S3).

MPK4 has been extensively studied in *Arabidopsis* and is known as the downstream signalling target of StMKK1; however, the role of AtMPK5 and its potato ortholog StMPK7 is not well studied for its role in immunity. Thus, we chose StMPK7 for further investigation. To further confirm the role of StMPK7 in potato defence against *P. infestans*, *GFP-StMPK7* was transformed into the potato cultivar Desirée via *Agrobacterium*-mediated transformation. Four independent transgenic lines were obtained and the enhanced expression of *StMPK7* in transgenic lines was detected by quantitative reverse transcription PCR (RT-qPCR) (Figure 2g). The transformants and control plants were grown over a period of 2 months and no developmental phenotypes were observed between the wild-type (WT) and *StMPK7*-overexpression (OE) lines (Figure 2h). The results of detached leaf assays showed that compared to the control plants, the *StMPK7*-OE lines developed smaller lesions at 4 days after inoculation with *P. infestans* (Figure 2i,j). These results confirm that overexpression of StMPK7 in potato enhances plant immunity to the late blight pathogen *P. infestans*.

2.3 | StMPK7 interacts with potato StMKK1 and is phosphorylated by this MAPKK

Both StMPK7 and StMPK4 participate in plant immunity and their *Arabidopsis* orthologs AtMPK4 and AtMPK5 are reported to be activated by AtMKK1/2 (Teige et al., 2004). The interaction between StMPK7 and StMKK1 was confirmed by yeast two-hybrid analysis. The results showed that StMPK7 strongly interacted with StMKK1

(Figure 4a). To further conform the interaction of StMKK1 with StMPK7, we performed coimmunoprecipitation assays (Co-IP) and firefly luciferase complementation imaging (LCI) assays. Results showed that myc-StMKK1 specifically coimmunoprecipitated with GFP-StMPK7 but not the negative control GFP (Figure 4b). For LCI assays, the results showed that the combination of StMPK7-nluc with cluc-StMKK1 restored the luciferase catalytic activity (Figure 4c), similar to the positive control GmBZR2-nluc and cluc-PP2C (Lu et al., 2017). To investigate whether StMPK7 is phosphorylated by StMKK1, we cloned *StMPK7* from the potato cultivar Tian11 into the pART-27 vector and fused an N-terminal GFP tag to the encoded protein. We transiently expressed the control GUS-myc or constitutively active (CA) StMKK1-myc (StMKK1$^{T220D, T226E}$), together with GFP-StMPK7, and checked the activation of the latter by phosphorylation, using anti-pERK antibodies. CA-StMKK1-myc was indeed found to phosphorylate StMPK7 (Figure 4d), indicating that in potato StMPK7 is phosphorylated by StMKK1 on activation of the corresponding MAPK cascade. To investigate whether StMPK7 is activated on treatment with flg22, we transiently expressed StMPK7 in *N. benthamiana* leaves and treated the plants with flg22 and determined whether StMPK7 was activated as a result of phosphorylation. Results showed that StMPK7 was indeed phosphorylated upon treatment with flg22 (Figure 4e). Similarly, the interaction of StMKK1 with StMPK4 was proved by Co-IP, and StMPK4 was found to be phosphorylated by the CA-StMKK1-myc (Figure S4a,b). The *NbMPK4*-silenced plants significantly reduced SA-related gene expression compared to control (Figure S4c).

To investigate whether *StMPK7* plays a role in the plant MTI response, we treated *N. benthamiana* plants, transiently overexpressing StMPK7, with flg22 and determined the expression levels of the MTI marker genes *FRK1* and *WRKY33*. Results showed that, when compared to the GUS control, StMPK7 overexpression significantly enhanced *FRK1* and *WRKY33* gene expression (Figure S5). Furthermore, to investigate the subcellular localization of StMPK7, we transiently expressed GFP-StMPK7 or GFP only in leaves of *N. benthamiana*, and at 2 days postinfiltration confocal microscopy was employed to observe the subcellular localization of StMPK7. The results showed that, similar to free GFP, GFP-StMPK7 showed both a nuclear and a cytoplasmic localization (Figure S6a). The integrity of the GFP-StMPK7 protein is shown in Figure S6b.

2.4 | Kinase activity of StMPK7 is required for promoting resistance to *P. infestans*

The self-activating mutation in the AtMPK4 protein (D198G, E202A), by which the protein becomes constitutively kinase-active, has been reported before (Berriri et al., 2012), and we performed a sequence alignment of AtMPK4 with potato, tomato, and *N. benthamiana* MPK7, of which the results showed that the D198 and E202 sites are conserved among these homologous proteins (Figure S7). We then generated a constitutively active mutant of StMPK7, referred to as CA-StMPK7-myc (StMPK7^{D198G,E202A}), to test whether the kinase
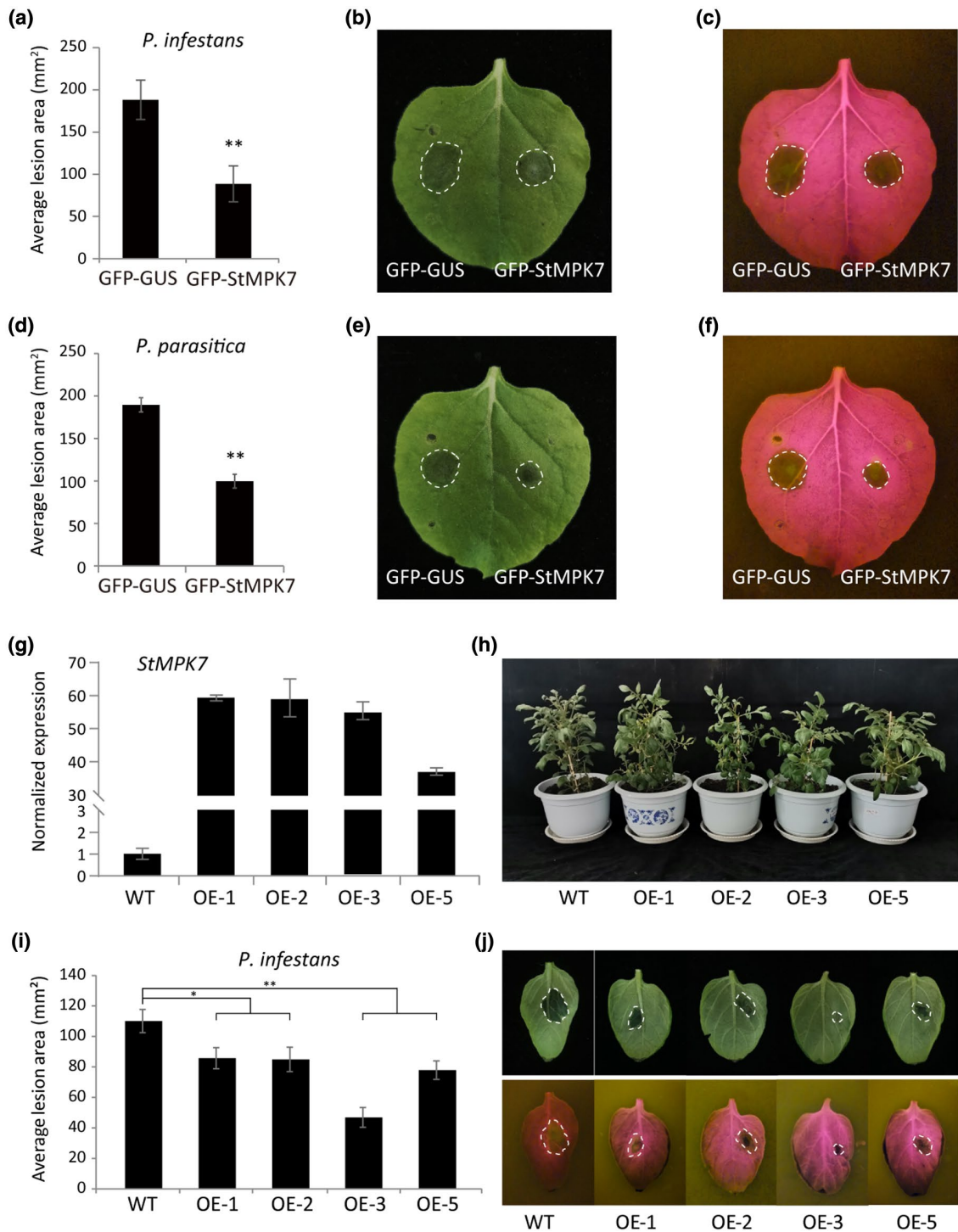
FIGURE 2 Overexpression of potato StMPK7 promotes resistance to *Phytophthora* pathogens. GFP-StMPK7 (right) and control GFP-GUS (left) were agroinfiltrated into *Nicotiana benthamiana* leaves. At 1 day postinfiltration (dpi), the *Phytophthora infestans* isolate 14–3-GFP (a, b, c) and *Phytophthora parasitica* isolate 1121 (d, e, f) were inoculated onto the leaves. The lesion diameters were measured at 5 days after inoculation (dai) for *P. infestans* and at 2 dai for *P. parasitica*, and average lesion areas (in mm^2) were calculated and are shown in (a) and (d), respectively. Representative images, taken under normal light (b, e) or blue light (c, f), show lesion development on GFP-GUS- and GFP-StMPK7-expressing leaves. (g) Quantitative reverse transcription PCR analysis shows *StMPK7* expression in wild-type (WT) and *StMPK7*-overexpressing (OE) plants. Lines OE-1, OE-2, OE-3, and OE-5 are independent transgenic lines. The expression level of *StActin* was used as an internal control and the WT value was used as the reference. (h) Plant morphology of 2-month-old WT and *StMPK7*-OE transgenic potato lines. (i) Graphs show the average lesion areas in mm^2 in WT and *StMPK7*-OE lines at 4 dai with *P. infestans*. (j) Representative images taken under normal (upper panel) or blue light (lower panel), showing lesion development on WT and *StMPK7*-OE lines at 4 dai. Error bars indicate the standard error from more than 10 technical replicates. Significant differences are indicated with asterisks (one-sided Student's *t* test, *$p < .05$, **$p < .01$). The experiments were repeated three times with similar results
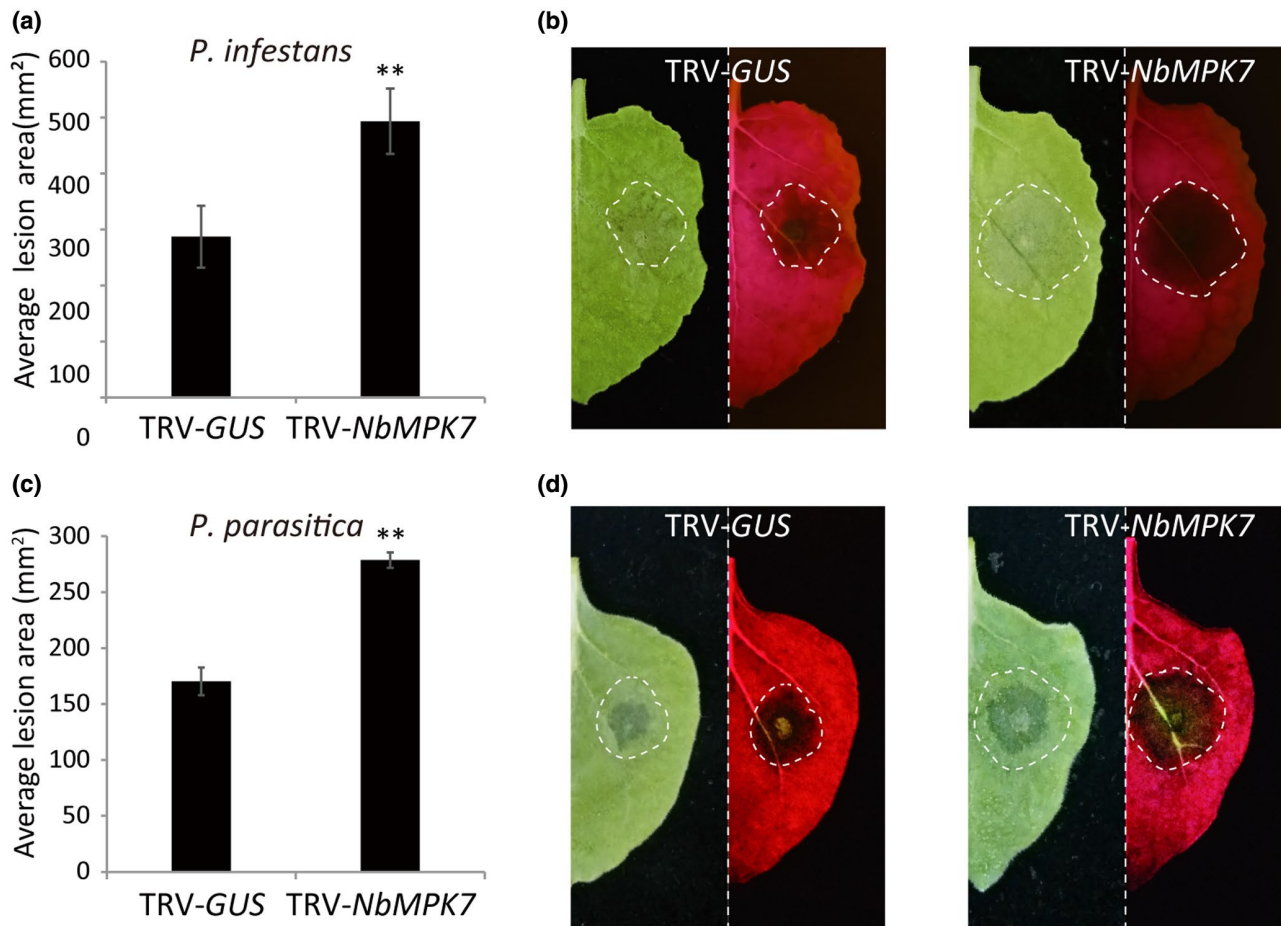
FIGURE 3 Silencing of *NbMPK7* promotes colonization by *Phytophthora* pathogens. Average lesion areas at 5 days after inoculation (dai) for *Phytophthora infestans* (a) and at 2 dai for *Phytophthora parasitica* (c) on TRV-*GUS*- and TRV-*NbMPK7*-inoculated plants are shown. The standard error from more than 10 technical replicates is indicated. Significant differences are indicated with asterisks (*n* ≥ 10; one-sided Student's *t* test, *p* ≤ .01). (b, d) Representative images taken under normal (left panel) or blue light (right panel), showing the lesion development on TRV-*GUS*- (left) and TRV-*NbMPK7*- (right) inoculated leaves. The experiments were repeated three times with similar results

activity of StMPK7 is required for defence against *Phytophthora* pathogens. The control GUS-myc and CA-StMPK7-myc were agro-infiltrated into the left and right panels of *N. benthamiana* leaves, respectively, and at 1 dpi *P. infestans* or *P. parasitica* was inoculated onto these panels. CA-StMPK7-myc overexpression significantly promoted resistance to both *P. infestans* and *P. parasitica* (Figure S8). The resistance provided by the constitutively active mutant CA-StMPK7-myc was much stronger than that triggered by wild-type StMPK7, and lesion formation by *P. infestans* was restricted to only the inoculation sites (Figure 5a,b). The accumulation of the myc- and GFP-tagged proteins was confirmed by western blotting (Figure 5c).

2.5 | Constitutively active (CA) StMPK7 induces cell death in *N. benthamiana* leaves

We observed that transient expression of CA-StMPK7-myc in leaves of *N. benthamiana* triggered a mild cell death starting from 3 dpi, after which the infiltrated region had completely dried out

at 5 dpi. At an OD_{600} of 0.7, CA-StMPK7-myc triggered 100% cell death at 5 dpi, while for an OD_{600} of 0.1, there was hardly any cell death observed (Figure 6a,b). To test whether transient expression of CA-StMPK7-myc induces reactive oxygen species (ROS) production, we performed 3,3′-diaminobenzidine (DAB) staining to visualize H_2O_2 accumulation. Results showed that in the CA-StMPK7-myc-expressing leaf half, significant amounts of H_2O_2 were generated when compared to the GUS-myc control (Figure 6c). To check whether the different severities of the cell death triggered by CA-StMPK7 were due to different levels of protein accumulation, we performed a western blot analysis with different OD_{600} of the infiltrated bacteria. Interestingly, wild-type StMPK7 accumulated at much higher levels than CA-StMPK7 at an OD_{600} of 0.1, and increasing the OD_{600} did not increase StMPK7 protein accumulation (Figure S9a). For CA-StMPK7, at an OD_{600} of 0.1 a weak band was detected and on an increase in OD_{600}, an enhanced accumulation of the CA-StMPK7 protein was observed (Figure S9b). However, with an OD_{600} above 0.7, protein accumulation was less, probably due to an enhanced and faster cell death taking place in the leaves.

(a)

**(b)**

(c)

(d)

(e)

FIGURE 4 Potato StMPK7 interacts with StMKK1 and is phosphorylated by this MAPKK. (a) Yeast coexpressing BD-StMKK1 and AD-StMPK7, and the positive control, did grow on quadruple drop-out (QDO) medium and yielded α-galactosidase activity, while the negative control and yeast coexpressing the empty vector BD with AD-StMPK7, or BD-StMKK1 with the empty vector AD, did not. (b) Coimmunoprecipitation (Co-IP) assays showed that StMKK1 associated with StMPK7. Green fluorescent protein (GFP) was used as negative control. Protein loading is indicated by Ponceau stain (Ponceau S). (c) Firefly luciferase complementation imaging (LCI) assays showed that StMPK7 interacts with StMKK1. GmBZR2-nluc and cluc-PP2C were used as positive control. Leaf samples were analysed and pictures were taken at 2–3 days postinfiltration using fluorescence imaging. (d) GFP-StMPK7 was transiently coexpressed with either GUS-myc or constitutively active CA-StMKK1-myc in *Nicotiana benthamiana* leaves. Total protein was extracted and the activation of GFP-StMPK7 through phosphorylation was detected by western blot, using α-pERK antibody. Ponceau S stain indicates the equal loading of the total protein extract. (c) Flg22-induced MAPK activation in GFP-StMPK7-overexpressing plants was detected by western blot, using α-pERK antibody. Leaves were treated with 10 μM flg22 and total proteins were extracted at 0 and 10 min after treatment

To investigate on which type of signalling components the cell death triggered by CA-StMPK7-myc depends, we silenced the *Suppressor of the G2 allele of Skp1* (*SGT1*, a chaperone-like protein generally required for *R* gene-mediated immunity), *Required for Mla12 resistance* (*RAR1*, encoding a co-chaperone of HSP90 required for ETI), the gene encoding the F-box protein Col1 (involved in JA activation), and the gene encoding the MPK4 downstream signalling component WRKY33, and subsequently infiltrated CA-StMPK7-myc. The cell death-inducer *P. infestans* elicitin INF1 and GUS-myc were included as controls. The results showed that CA-StMPK7-myc-triggered cell death was abolished in *SGT1*- and *RAR1*-silenced plants, and was partially suppressed in *WRKY33*-silenced plants, whereas Col1 appeared to play a less important role in the activation of cell death by CA-StMPK7 (Figure 6d).

2.6 | StMPK7 promotes potato resistance to *Phytophthora* pathogens via SA-related immune signalling

Although SGT1 and RAR1 participate in multiple cellular processes, they are essential for *R* gene-mediated immunity that largely depends on the hormone salicylic acid (SA) (Zhang & Li, 2019). Indeed, silencing of *SGT1* has been reported earlier to reduce SA-responsive gene expression (Rong et al., 2010). We thus investigated whether CA-StMPK7-myc-triggered cell death depends on SA. SA is a key plant hormone regulating defence to *Phytophthora* pathogens (Zhou et al., 2018). We tested SA-related marker gene expression in *N. benthamiana* leaves transiently expressing StMPK7. For this, GFP-StMPK7 and the control GFP-GUS were transiently expressed in *N. benthamiana* leaves, and at 2 days after agroinfiltration the leaves were harvested for RNA extraction. Expression of the SA-related genes *Pathogenesis-related (PR) protein-1* and *PR-2* was detected by RT-qPCR, and we observed that overexpression of *StMPK7* promoted *NbPR-1* and *NbPR-2* gene expression in *N. benthamiana* (Figure 7a). The SA-related marker gene expression in potato *StMPK7*-OE lines was also tested by RT-qPCR, and results showed that in potato *StMPK7*-OE transgenic lines the *StPR1* and *StPR2* gene expression was significantly enhanced compared to the control plants (Figure 7a). To test whether the cell death triggered
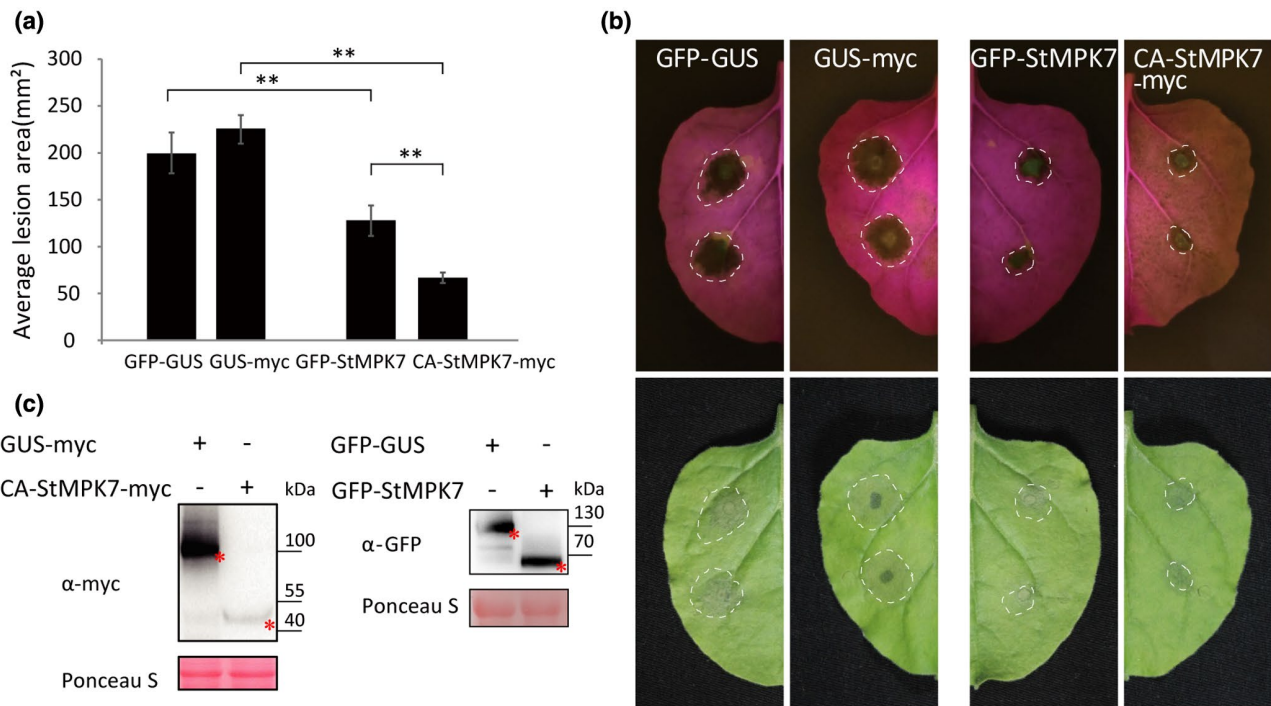
FIGURE 5 Overexpression of constitutively active (CA)StMPK7 confers stronger resistance to *Phytophthora infestans* than overexpression of wild-type (WT) StMPK7. (a) Green fluorescent protein (GFP)-β-glucuronidase (GUS), GUS-myc, GFP-StMPK7, and CA-StMPK7-myc were agroinfiltrated into *Nicotiana benthamiana* leaves. At 1 day postinfiltration (dpi), *P. infestans* isolate 14-3-GFP was inoculated at the agroinfiltrated sites. The lesion diameter was measured at 5 days after inoculation (dai) and average lesion areas were calculated and are shown in the graph. (b) Representative images taken under normal light (lower panel) or blue light (upper panel) show lesion development as a result of infection by *P. infestans* on *N. benthamiana* leaves. Error bars show the standard error from more than 10 technical replicates. Significant differences are indicated with asterisks ($n \geq 10$; one-sided Student's t test, $p \leq .01$). The experiment was repeated three times, with similar results. (c) The accumulation of CA-StMPK7-myc, GUS-myc, GFP-GUS, and GFP-StMPK7 proteins is shown by western blot and the expected protein bands are marked with red asterisks

by CA-StMPK7 also requires SA-related signalling, we coexpressed the salicylate hydroxylase *NahG* gene with CA-StMPK7 and checked whether the cell death response was altered. Again, the *P. infestans* elicitin INF1 was used as a cell death control. Results showed that coexpression of NahG significantly suppressed the CA-StMPK7-triggered cell death, whereas the INF1-triggered cell death was not altered by NahG coexpression (Figure 7b). The H_2O_2 accumulation at the sites agroinfiltrated with CA-StMPK7, either in combination with GUS or with NahG, was measured by DAB staining. We observed that a significant amount of H_2O_2 was generated at the sites where CA-StMPK7 and GUS were coexpressed and at the sites were INF1 and GUS/NahG were coexpressed, whereas the expression of NahG significantly repressed the CA-StMPK7-triggered H_2O_2 accumulation (Figure 7b). The repression of CA-StMPK7-triggered cell death by NahG was quantified by ion leakage assays. The reduced ion leakage that we observed confirmed that NahG significantly repressed CA-StMPK7-triggered cell death (Figure 7c).

3 | DISCUSSION

In this study, we describe the identification and characterization of potato StMPK7 as a downstream signalling target of StMKK1

(Figure 1). We show that the StMKK1 interacted with and phosphorylated StMPK7 (Figure 4). StMPK7 and StMPK4 both positively regulated immunity against *Phytophthora* pathogens (Figures 2, 3, S1, and S2) and the constitutively active mutant CA-StMPK7 enhanced resistance to *Phytophthora* pathogens (Figures 5 and S8) and triggered an SGT1/RAR1-dependent cell death (Figure 6). Further investigations revealed that overexpression of StMPK7 enhanced pathogenesis-related gene expression (Figure 7), whereas CA-StMPK7-induced cell death was strongly repressed by the SA hydroxylase NahG (Figure 7). Thus, we conclude that potato StMPK7 and StMPK4 function as downstream signalling components of the phosphorelay cascade initiated by StMKK1, which enhances resistance to *Phytophthora* pathogens by triggering SA-dependent immunity. Phylogenetic analysis of StMPK7 showed that *Arabidopsis* AtMPK4/5/11/12 group together with three MPKs of *Populus*, two of *Oryza*, and three of tomato and potato. These subclade B MPKs have undergone complicated gene duplication and gene loss processes. StMPK7 and StMPK4 are functional orthologs of *AtMPK4/5/11/12* (Figure 1). Because StMKK1 interacted with and phosphorylated StMPK7 (Figure 4), just like *Arabidopsis* AtMKK1 interacts with and phosphorylates AtMPK4 (Bi et al., 2018), we conclude that StMPK7 is a downstream signalling component of StMKK1. Thus, potato probably has a StMKK1-StMPK7 phosphorelay cascade, similar to

the *Arabidopsis* MKK1-MPK4 cascade. StMPK7 was phosphorylated on MTI activation, and overexpression of StMPK7 promoted MTI-related gene expression (Figure S5), indicating that the StMKK1-StMPK7 cascade positively regulates MTI.

Transient expression of StMPK7 and CA-StMPK7 in *N. benthamiana* enhanced resistance to *Phytophthora* pathogens (Figures 2, 5, and S8). Furthermore, resistance conferred by CA-StMPK7 was much stronger than that provided by wild type StMPK7 (Figure 5). These results indicate that the kinase activity of StMPK7 is important
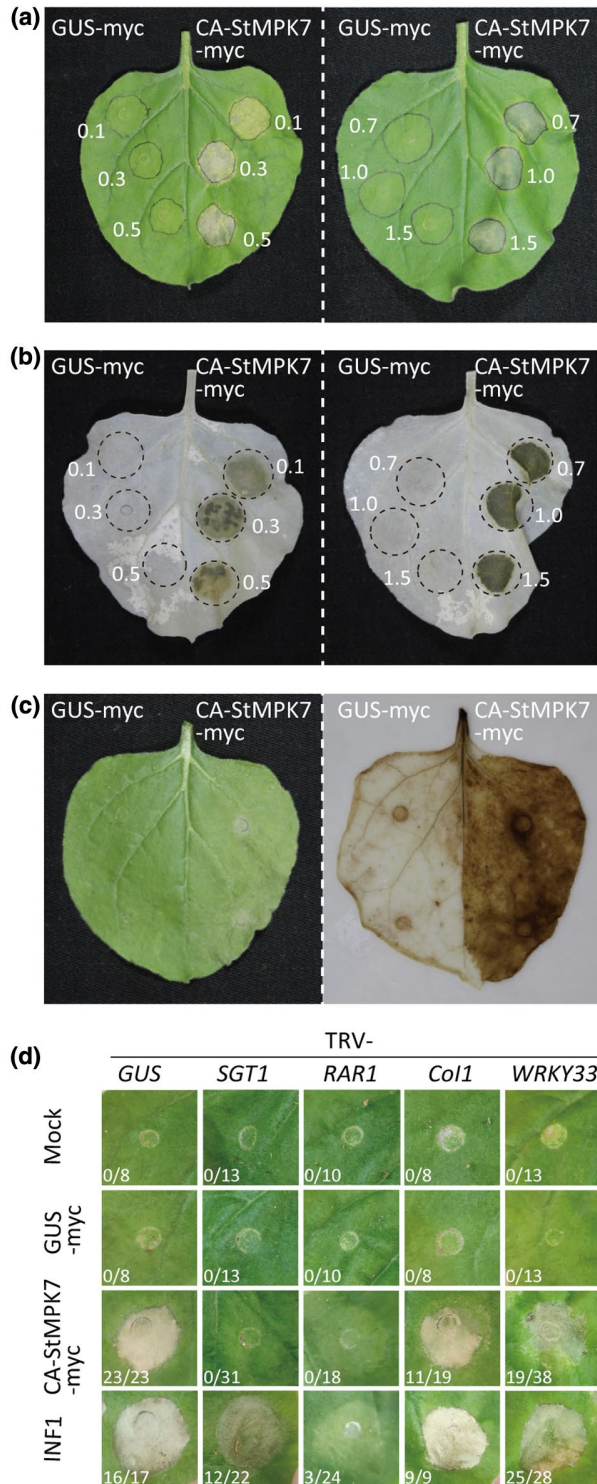
FIGURE 6 Overexpression of constitutively active (CA) StMPK7 triggers an SGT1/RAR1-dependent cell death in *Nicotiana benthamiana* leaves. (a) Cell death triggered by CA-StMPK7-myc in leaves of *N. benthamiana*. The number next to the infiltrated zone indicates the OD_{600} of the agrobacterial suspension used for agroinfiltration. (b) Cell death triggered by CA-StMPK7-myc is visible as dark spots in the leaves from which the chlorophyll was removed by treatment with ethanol. (c) 3,3′-diaminobenzidine (DAB) staining revealing reactive oxygen species accumulation at the CA-StMPK7-myc-infiltrated sites. (d) SGT1 and RAR1 are required for CA-StMPK7-myc-triggered cell death. Three weeks after inoculation to initiate virus-induced silencing of *SGT1* or *RAR1*, the negative control GUS-myc, the cell death inducer INF1, and CA-StMPK7-myc were agroinfiltrated at an OD_{600} of 1.0 into the middle leaves of silenced plants. Pictures were taken at 5 days postinfiltration (dpi). The ratios next to the infiltrated zones show the number of infiltration sites showing cell death versus the total amount of infiltrated sites from two independent experiments at 5 dpi

for plant immunity. In *Arabidopsis*, an *mpk4* knock-out mutant shows an autoimmune phenotype and, therefore, AtMPK4 was suggested to be a negative regulator of immunity (Kong et al., 2012). However, later it was reported to be a positive regulator of immunity through participating in the MTI response (Bi et al., 2018; Zhang et al., 2017). The autoimmune response of the *mpk4* knock-out mutant was in fact caused by the activation of the NLR protein SUMM2, which guards the MEKK1-MKK1/2-MPK4 proteins taking part in this phosphorelay cascade and confers *R* gene-mediated immunity when this cascade is being manipulated, either by microbial pathogens or by mutations (Zhang et al., 2012, 2017). This finding is supported by the observation that the *Pseudomonas syringae* effector HopAI1 triggers plant immunity by inactivating MPK4 (Zhang et al., 2012). However, in our study on silencing of *NbMPK4/7* the plants become more susceptible to *Phytophthora* pathogens, instead of more resistant (Figure 3). This observation indicates that in solanaceous plants there is probably no SUMM2-like NLR protein guarding the StMKK1-StMPK7 cascade.

Both StMPK7 and StMPK4 promote resistance, which was reflected by the reduced lesion areas in leaf tissue overexpressing these MAPKs when compared to overexpression of the GFP-GUS control (Figures 2 and S1). StMKK1 interacted with and phosphorylated both StMPK7 and StMPK4 (Figures 4 and S4). StMPK7 was activated by flg22 treatments (Figure 4) just as reported for MPK4 (Gao et al., 2008), and both StMPK7 and MPK4 participated in SA-related signalling pathway (Figures 7 and S4c). Taken together with the fact that silencing either NbMPK4 or NbMPK7 hampered plant immunity to *Phytophthora* pathogens (Figures 3 and S2), this indicates that they are not simply functional redundant genes. Instead, probably StMPK4 and StMPK7 function collaboratively downstream of StMKK1. Potato has six MKKs and 21 MPK proteins (Iftikhar et al., 2017), so probably several MPKs work downstream of one MKK. In our research we identified that besides StMPK4, StMPK7 also works downstream of StMKK1, and StMPK4 and StMPK7 show overlapping but nonredundant functions in plant immunity. Probably plants employ multiple MPK proteins to amplify the immune signalling. Our results showed
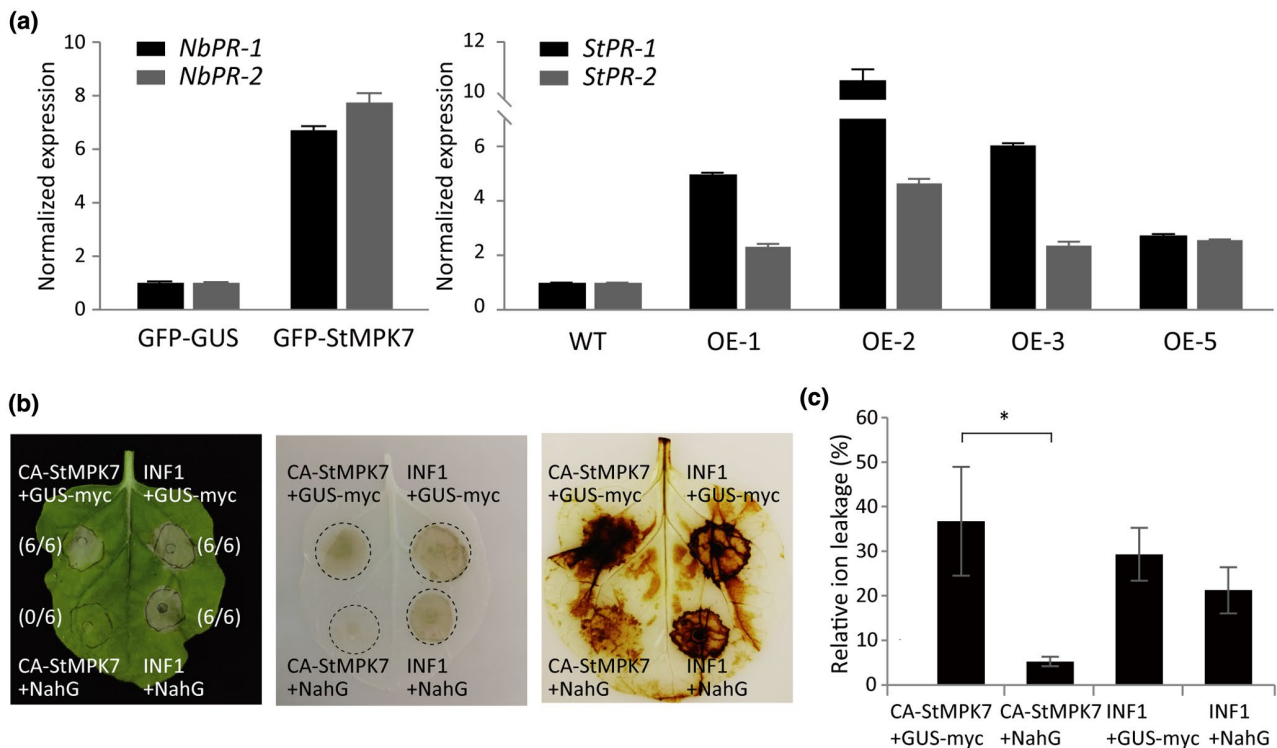
FIGURE 7 StMPK7 promotes plant resistance via salicylic acid (SA)-related immune signalling. (a) StMPK7 promotes plant SA-related gene expression. Graphs show the relative expression of *NbPR-1*, *NbPR-2* in green fluorescent protein (GFP)-β-glucuronidase (GUS)-, and GFP-StMPK7-overexpressing (OE) *Nicotiana benthamiana* leaves and *StPR-1*, *StPR-2* in wild-type (WT) and *StMPK7*-OE stable transgenic potato lines. The expression of the *NbActin* gene and the *StActin* gene was used for normalization. Gene expression levels in GFP-StMPK7-expressing plants and stable *StMPK7*-OE transgenic potato plants were significantly higher than those in the control plants. The experiments were repeated twice, with similar results. (b) CA-StMPK7-myc-triggered cell death is compromised by coexpression with the salicylate hydroxylase NahG. The left picture shows cell death triggered by CA-StMPK7-myc and INF1 when coexpressed with GUS-myc or NahG. The ratios next to the infiltrated zones show the amount of infiltrated sites showing cell death versus the total amount of infiltrated sites from two independent experiments at 5 days postinoculation (dpi). Pictures were taken at 5 dpi. The middle picture shows cell death as dark spots in the leaves from which chlorophyll was removed by treatment with ethanol. The right picture shows the H_2O_2 accumulation at the infiltrated sites with 3,3′-diaminobenzidine (DAB) staining. (c) Quantification of cell death triggered by CA-StMPK7 and INF1 by ion leakage assays. CA-StMPK7 and INF1 were coexpressed with either GUS-myc or NahG, and the amount of cell death was quantified by ion leakage assays. The relative ion leakage values were measured at 5 dpi. Error bars indicate the *SD*

that resistance conferred by CA-StMPK7 was stronger than that provided by *StMPK7*, as is apparent from the severely restricted lesions that developed at the inoculation sites (Figure 5). Moreover, CA-StMPK7 triggered a mild cell death at 3 dpi when agroinfiltrated at an OD_{600} of 0.3 or higher (Figure 6). Thus, the cell death triggered by CA-StMPK7 is probably due to the overactivation of immune signalling downstream of StMPK7.

AtMPK4 has been reported to sequester the transcription factor WRKY33 to the cytoplasm in the resting state, whereas on activation of MTI, WRKY33 is released from AtMPK4, allowing it to move to the nucleus and to activate a number of genes that is required for camalexin biosynthesis (Zhou et al., 1999). Our results showed that WRKY33 played a minor role in CA-StMPK7-triggered cell death (Figure 6d), which may be due to the fact that this transcription factor is probably not the key signalling component downstream of StMPK7 in regulating host immunity. WRKY33 was not accountable for the MPK4-regulated hormone-responsive gene expression (Qiu et al., 2008), and AtMPK4 has multiple putative substrates besides

WRKY33 (Zhang, Chhajed, et al., 2019; Zhang, Schneider, et al., 2019). Furthermore, there is a plethora of *WRKY* genes in plants, and the minor involvement of WRKY33 in CA-StMPK7-triggered cell death may be due to redundancy of the various WRKYs.

SGT1 and RAR1 are involved in multiple cellular processes. However, most importantly, they are involved in *R* gene-mediated immunity, which largely depends on SA-signalling (Zhang & Li, 2019). We observed that overexpression of *StMPK7* significantly enhanced *PR1* and *PR2* gene expression (Figure 7a), typically reflecting SA-related gene expression, and the presence of the salicylate hydroxylase NahG significantly repressed CA-StMPK7-triggered cell death (Figure 7b,c), supporting the notion that StMPK7-mediated immune signalling requires the accumulation of SA. MAPK cascades are generally known to participate in plant MTI and ETI responses and trigger the alteration of plant hormone levels, such as that of SA (Kawano et al., 2010; Zhang et al., 2012, 2018). This also supports our findings that the StMKK1-StMPK7 cascade enhances plant immunity via SA-dependent signalling.

In summary, our research identified the potato *MPK4/5*-orthologous genes *StMPK4/6* and *StMPK7*, and we have provided evidence that a functional StMKK1-StMPK7 phosphorelay cascade exists in potato and functions in MTI. StMPK7 was shown to activate SA-related immunity, and cell death triggered by constitutively active StMPK7 depends on SA signalling. Our work adds to the studies on MAPK cascades in crop plants and provides evidence for the functioning of MAPK cascades in SA-related immunity.

4 | EXPERIMENTAL PROCEDURES

4.1 | Plasmid construction

The open reading frames (ORFs) of *StMPK7* (*PGSC0003DMC400021542*), *StMPK6* (*PGSC0003DMP400037535*), and *StMPK4* (*PGSC0003DMP400000144*) were cloned by performing a PCR employing the primer pairs shown in Table S1, using a cDNA library from potato cultivar Tian11 as a template. The amplified fragments were inserted into the pART27-NGFP, pART27-Nmyc, pART27-CGFP, and pART27-Cmyc vectors using *Eco*RI and *Xba*I sites present in the primers to generate the *GFP-StMPK7*, *GFP-StMPK6*, *myc-StMKK1*, *StMPK4-GFP*, and *StMPK4-myc* plasmids. The constitutively active (CA) mutants *CA-StMPK7-myc* (*StMPK7^{D198G,E202A}*) and *CA-StMKK1-myc* (*StMKK1^{T220D,T226E}*) were generated by overlap extension PCR using *GFP-StMPK7* and *GFP-StMKK1* as templates, respectively, with the primers shown in Table S1, and cloned into the pART27-cmyc vector using *Xho*I and *Eco*RI sites (Fan et al., 2018). For yeast two-hybrid assays, *StMPK7* was cloned into the pGADT7 vector using the *Eco*RI and *Bam*HI sites to generate the pGADT7:*StMPK7* plasmid. For firefly luciferase complementation imaging (LCI) assays, StMPK7 and StMKK1 were cloned into pCAMBIA-nLuc and pCAMBIA-cLuc vectors using *Kpn*I and *Sal*I sites to form the StMPK7-nluc and cluc-StMKK1 plasmids, respectively.

4.2 | Plant growth conditions and detached leaf assays

N. benthamiana and potato plants were grown in a climate chamber with a 16 hr light and 8 hr dark cycle at 25 °C, and with a relative humidity (RH) of 45%. The middle two or three fully expanded leaves from 4- to 5-week-old *N. benthamiana* plants were detached and used for infection assays. For this, *P. infestans* 14-3-GFP and *P. parasitica* isolate 1121 were grown as described by Li et al. (2019) and zoospores were harvested and used for inoculation. Ten microlitres of a 1×10^5/ml zoospore suspension of *P. infestans* and 10 µl of a 2×10^5/ml zoospore suspension of *P. parasitica* were used for inoculation. *P. infestans*- and *P. parasitica*-inoculated leaves were incubated at 100% RH at 18 °C for 5 or 6 days, and at 23 °C for 2 or 3 days, respectively, before the diameters of the lesions were measured.

4.3 | Agroinfiltration

GFP-StMPK7 and *CA-StMPK7-myc* were transformed into the *Agrobacterium* strain C58C1, and the bacteria were gown at 28 °C in liquid Luria-Bertani medium with the antibiotics tetracycline and spectinomycin for 2 days. Then the bacterial suspension was centrifuged at $1,000 \times g$, the cells were resuspended in infiltration medium (Champouret et al., 2009), and the density was adjusted to an OD_{600} of 0.1 for assays involving confocal microscopy and infection assays, OD_{600} of 0.3 for co-immunoprecipitations (Co-IPs), and OD_{600} of 0.7 for cell death assays.

4.4 | Virus-induced gene silencing

To select the target sequence of *NbMPK7* for virus-induced gene silencing (VIGS) assays, we BLAST searched the *PGSC0003DMC400021542* gene sequence in the Sol genomics network database (https://solgenomics.net/) and identified two genes, *Niben101Scf00254g02007.1* (*NbMPK7a*) and *Niben101Scf00421g01029.1* (*NbMPK7b*), both encoding a *NbMPK7* ortholog in *N. benthamiana*. We selected one cDNA fragment targeting both genes for generating the tobacco rattle virus (TRV)-*NbMPK7* vector. The TRV-*NbMPK4/6* constructs were generated in a similar way using the primer pairs shown in Table S1. TRV-*GUS* was used as a negative control in our VIGS assays. *Agrobacterium* strain C58C1, containing either TRV1 (TRV-RNA1) or TRV2 (TRV-RNA2) (Ryu et al., 2004), was cultured, centrifuged, and resuspended in infiltration medium before being mixed in a 1:1 ratio to a final OD_{600} of 1. The first two leaves of 2-week-old *N. benthamiana* plants were used for agroinfiltration of the TRV-*NbMPK7/4/6* constructs. Three weeks after infiltration, the fifth and sixth leaves counted from the bottom were selected for infection assays.

4.5 | Potato transformation

Agrobacterium strain GV3101, harbouring the GFP-StMPK7 plasmid, was transformed into potato cultivar Desirée as described by Sun et al. (2016). Rooted transformants were transferred to Murashige & Skoog plates without antibiotics and were cultured for 3 weeks in a climate chamber with a 16 hr light and 8 hr dark cycle at 23 °C before being planted in potting soil.

4.6 | Firefly LCI assay

The firefly LCI assays were performed according to the protocol described by Chen et al. (2008).

4.7 | Flg22 treatments and ROS production assays

A 10 µM flg22 solution in water was infiltrated into the leaves of *N. benthamiana*. After 3 hrs of flg22 treatment , leaves were

harvested for checking of MTI marker gene expression. ROS production assays were performed according to the method described by Li et al. (2016).

4.8 | Kinase activation assay

GFP-StMPK7 was coexpressed with CA-StMKK1-myc or the control GUS-myc by transient transformation of *N. benthamiana* leaves. Proteins were extracted using an extraction buffer with phosphatase inhibitor cocktails 2 and 3 (Sigma). The activation of StMPK7 through phosphorylation was detected using anti-pERK antibody (Phospho-p44/42 MAPK [Erk1/2] [Thr202/Tyr204]; Cell Signaling Technology).

4.9 | Gene expression assays

TRIzol reagent (Invitrogen) was used for total RNA extraction, and first-strand cDNA was synthesized from 1 μg of total RNA according to the manufacturer's instructions (PrimeScript RT reagent Kit; TaKaRa). For each PCR, 5 μl of the 20 times diluted cDNA was used as a template and SYBR Green master mix (Roche) was used. An iQ7 Real-Time Cycler (Life Technologies) was used to run RT-qPCRs. Gene expression was quantified and normalized to the *N. benthamiana* housekeeping gene *actin* using the $\Delta\Delta C_t$ method. Primer pairs for testing gene silencing efficiency were designed beyond the VIGS-targeting sequence (Table S1).

4.10 | Coimmunoprecipitation and western blot assays

Total proteins were extracted using GTEN buffer as described by Du et al. (2021). For Co-IP assays, for each 1.6 ml of total protein extraction a 12 μl of GFP-trap_A beads (Chromotek) were added, and the mixtures were incubated for 2 hr with gentle shaking at 4 °C before proteins were spun down. The beads were washed with protein extraction buffer five times before being boiled in protein loading buffer. For western blot assays, proteins were separated on 10% sodium dodecyl sulphate (SDS)-polyacrylamide gels and subsequently transferred to Immune-Blot PVDF membranes (Roche). The membranes were blocked in 10 ml of blocking buffer (TBST; Tris-buffered saline pH 7.2, 0.05% Tween 20 [Sigma]) containing 5% of nonfat milk, with gentle shaking for 2 hr at room temperature. Subsequently, membranes were incubated with anti-GFP (#AE012, ABclonal), anti-myc (#AE010, ABclonal), or anti-pERK antibody at the appropriate dilution for 1.5–2 hr with gentle shaking at room temperature. Then the membranes were washed five times and incubated with the secondary antibodies horseradish peroxidase-conjugated goat anti-rabbit IgG (H + L) antibody (#AS014, ABclonal) for another 1.5–2 hr. After this incubation, membranes were washed with TBST five times before proteins were detected (eECL western blot kit; CWBio).

4.11 | Yeast two-hybrid assays

The binding domain (BD) plasmid pGBKT7:*StMKK1*, or the empty vector pGBKT7, and the activation domain (AD) plasmid pGADT7:*StMPK7*, or empty vector pGADT7, were cotransformed into *Saccharomyces cerevisiae* AH109 (Li et al., 2019). Transformations were checked on selective drop-out (SD)/−Trp−Leu medium and interactions were confirmed on QDO (SD/−Trp−Leu−His−Ade) medium, together with a gain of α-galactosidase activity (α-gal), by adding X-α-Gal in QDO medium. Yeast controls showing either positive or negative interaction were provided by the Matchmaker GAL4 Two-Hybrid System 3 (Clontech).

4.12 | Confocal microscopy

An IX83 confocal microscope (Olympus Life Science) was used to determine the subcellular localization of GFP-StMPK7. GFP was excited at a wavelength of 488 nm and the emission was detected between 500 and 540 nm. Images were processed with Olympus Fluoview and figures were generated using Adobe Illustrator.

4.13 | DAB staining and ion leakage assays

Leaves were incubated with a DAB staining solution (1 mg/ml, DAB dissolved in Milli-Q water with addition of HCl to adjust the pH to 3.7) overnight, and then washed with water before pictures were taken. Ion leakage assays were performed as described by Bouwmeester et al. (2014).

AUTHOR CONTRIBUTIONS
Y.D. and W.S. designed the research. H.Z., F.L., Z.L., J.C., and X.C. performed the experiments. Y.D. and H.Z. analysed the data. Q.W. built the phylogenetic tree. Y.D., M.H.A.J.J., and W.S. wrote the manuscript. All authors reviewed the manuscript.

DATA AVAILABILITY STATEMENT
Research data are not shared.

ORCID

Houxiao Zhang https://orcid.org/0000-0003-4800-293X
Fangfang Li https://orcid.org/0000-0001-6722-0698
Xiaokang Chen https://orcid.org/0000-0003-1921-0991
Qinhu Wang https://orcid.org/0000-0003-1251-073X
Matthieu H.A.J. Joosten https://orcid.org/0000-0002-6243-4547
Weixing Shan https://orcid.org/0000-0001-7286-4041
Yu Du https://orcid.org/0000-0002-3512-0200

REFERENCES

Asai, T., Tena, G., Plotnikova, J., Willmann, M.R., Chiu, W.L., Gomez-Gomez, L. et al. (2002) MAP kinase signalling cascade in Arabidopsis innate immunity. *Nature*, 415977–983. https://doi.org/10.1038/415977a

Berriri, S., Garcia, A.V., Frei dit Frey, N., Rozhon, W., Pateyron, S., Leonhardt, N. et al. (2012) Constitutively active mitogen-activated protein kinase versions reveal functions of Arabidopsis MPK4 in pathogen defense signaling. *The Plant Cell*, 24, 4281–4293. https://doi.org/10.1105/tpc.112.101253

Bi, G., Zhou, Z., Wang, W., Li, L., Rao, S., Wu, Y. et al. (2018) Receptor-like cytoplasmic kinases directly link diverse pattern recognition receptors to the activation of mitogen-activated protein kinase cascades in Arabidopsis. *The Plant Cell*, 30, 1543–1561. https://doi.org/10.1105/tpc.17.00981

Bouwmeester, K., Han, M., Blanco-Portales, R., Song, W., Weide, R., Guo, L. et al. (2014) The *Arabidopsis* lectin receptor kinase LecRK-I.9 enhances resistance to *Phytophthora infestans* in solanaceous plants. *Plant Biotechnology Journal*, 12, 10–16. https://doi.org/10.1111/pbi.12111

Chai, J., Liu, J., Zhou, J. & Xing, D. (2014) Mitogen-activated protein kinase 6 regulates *NPR1* gene expression and activation during leaf senescence induced by salicylic acid. *Journal of Experimental Botany*, 65, 6513–6528. https://doi.org/10.1093/jxb/eru369

Champouret, N., Bouwmeester, K., Rietman, H., van der Lee, T., Maliepaard, C., Heupink, A. et al. (2009) Phytophthora infestans isolates lacking class I ipiO variants are virulent on *Rpi-blb1* potato. *Molecular Plant-Microbe Interactions*, 22, 1535–1545. https://doi.org/10.1094/MPMI-22-12-1535

Chen, H., Zou, Y., Shang, Y., Lin, H., Wang, Y., Cai, R. et al. (2008) Firefly luciferase complementation imaging assay for protein–protein interactions in plants. *Plant Physiology*, 146, 368–376. https://doi.org/10.1104/pp.107.111740

Du, Y., Berg, J., Govers, F. & Bouwmeester, K. (2015) Immune activation mediated by the late blight resistance protein R1 requires nuclear localization of R1 and the effector AVR1. *New Phytologist*, 207, 735–747. https://doi.org/10.1111/nph.13355

Du, Y., Chen, X., Guo, Y., Zhang, X., Zhang, H., Li, F. et al. (2021) *Phytophthora infestans* RXLR effector PITG20303 targets a potato MKK1 protein to suppress plant immunity. *New Phytologist*, 229, 501–515. https://doi.org/10.1111/nph.16861

Engelhardt, S., Boevink, P.C., Armstrong, M.R., Ramos, M.B., Hein, I. & Birch, P.R.J. (2012) Relocalization of late blight resistance protein R3a to endosomal compartments is associated with effector recognition and required for the immune response. *The Plant Cell*, 24, 5142–5158. https://doi.org/10.1105/tpc.112.104992

Fan, G., Yang, Y., Li, T., Lu, W., Du, Y.U., Qiang, X. et al. (2018) A *Phytophthora capsici* RXLR effector targets and inhibits a plant PPIase to suppress endoplasmic reticulum-mediated immunity. *Molecular Plant*, 11, 1067–1083. https://doi.org/10.1016/j.molp.2018.05.009

Frei dit Frey, N., Garcia, A., Bigeard, J., Zaag, R., Bueso, E., Garmier, M. et al. (2014) Functional analysis of *Arabidopsis* immune-related

MAPKs uncovers a role for MPK3 as negative regulator of inducible defences. *Genome Biology*, 15, R87. https://doi.org/10.1186/gb-2014-15-6-r87

Fry, W. (2008) *Phytophthora infestans*: The plant (and *R* gene) destroyer. *Molecular Plant Pathology*, 9, 385–402. https://doi.org/10.1111/j.1364-3703.2007.00465.x

Gao, M., Liu, J., Bi,, D., Zhang, Z., Cheng, F. & Chen, S. (2008) MEKK1, MKK1/MKK2 and MPK4 function together in a mitogen-activated protein kinase cascade to regulate innate immunity in plants. *Cell Research*, 18, 1190–1198. https://doi.org/10.1038/cr.2008.300

Hettenhausen, C., Baldwin, I.T. & Wu, J. (2013) *Nicotiana attenuata* MPK4 suppresses a novel jasmonic acid (JA) signaling-independent defense pathway against the specialist insect *Manduca sexta*, but is not required for the resistance to the generalist *Spodoptera littoralis*. *New Phytologist*, 199, 787–799. https://doi.org/10.1111/nph.12312

Hou, X., Ding, L. & Yu, H. (2013) Crosstalk between GA and JA signaling mediates plant growth and defense. *Plant Cell Reports*, 32, 1067–1074. https://doi.org/10.1007/s00299-013-1423-4

Ichimura, K., Shinozaki, K., Tena, G., Sheen, J., Henry, Y., Champion, A. et al. (2002) Mitogen-activated protein kinase cascades in plants: A new nomenclature. *Trends in Plant Science*, 7, 301–308. https://doi.org/10.1016/S1360-1385(02)02302-6

Iftikhar, H., Naveed, N., Virk, N., Bhatti, M.F. & Song, F. (2017) *In silico* analysis reveals widespread presence of three gene families, MAPK, MAPKK and MAPKKK, of the MAPK cascade from crop plants of Solanaceae in comparison to the distantly-related syntenic species from Rubiaceae, coffee. *PeerJ*, 5, e3255. https://doi.org/10.7717/peerj.3255

Jagodzik, P., Tajdel-Zielinska, M., Ciesla, A., Marczak, M. & Ludwikow, A. (2018) Mitogen-activated protein kinase cascades in plant hormone signaling. *Frontiers in Plant Science*, 9, 1387. https://doi.org/10.3389/fpls.2018.01387

Jones, J.D. & Dangl, J.L. (2006) The plant immune system. *Nature*, 444, 323–329. https://doi.org/10.1038/nature05286

Kandoth, P.K., Ranf, S., Pancholi, S.S., Jayanty, S., Walla, M.D., Miller, W. et al. (2007). Tomato MAPKs LeMPK1, LeMPK2, and LeMPK3 function in the systemin-mediated defense response against herbivorous insects. *Proceedings of the National Academy of Sciences of the United States of America*, 104, 12205–12210. https://doi.org/10.1073/pnas.0700344104

Kawano, Y., Akamatsu, A., Hayashi, K., Housen, Y., Okuda, J., Yao, A.I. et al. (2010) Activation of a Rac GTPase by the NLR family disease resistance protein Pit plays a critical role in rice innate immunity. *Cell Host & Microbe*, 7, 362–375. https://doi.org/10.1016/j.chom.2010.04.010

King, S.R., McLellan, H., Boevink, P.C., Armstrong, M.R., Bukharova, T., Sukarta, O. et al. (2014) *Phytophthora infestans* RXLR effector PexRD2 interacts with host MAPKKKε to suppress plant immune signaling. *The Plant Cell*, 26, 1345–1359. https://doi.org/10.1105/tpc.113.120055

Kong, Q., Qu, N., Gao, M., Zhang, Z., Ding, X., Yang, F. et al. (2012) The MEKK1-MKK1/MKK2-MPK4 kinase cascade negatively regulates immunity mediated by a mitogen-activated protein kinase kinase kinase in *Arabidopsis*. *The Plant Cell*, 24, 2225–2236. https://doi.org/10.1105/tpc.112.097253

Li, T., Wang, Q., Feng, R., Li, L., Ding, L., Fan, G. et al. (2019) Negative regulators of plant immunity derived from cinnamyl alcohol dehydrogenases are targeted by multiple *Phytophthora* Avr3a-like effectors. *New Phytologist*, https://doi.org/10.1111/nph.16139

Li, X., Zhang, Y., Huang, L., Ouyang, Z., Hong, Y., Zhang, H. et al. (2014) Tomato SlMKK2 and SlMKK4 contribute to disease resistance against *Botrytis cinerea*. *BMC Plant Biology*, 14, 166. https://doi.org/10.1186/1471-2229-14-166

Li, Y., Chang, Y., Zhao, C., Yang, H. & Ren, D. (2016) Expression of the inactive ZmMEK1 induces salicylic acid accumulation and salicylic

acid-dependent leaf senescence. *Journal of Integrative Plant Biology*, 58, 724–736. https://doi.org/10.1111/jipb.12465

Lu, X., Xiong, Q., Cheng, T., Li, Q.-T., Liu, X.-L., Bi, Y.-D. et al. (2017) A PP2C-1 allele underlying a quantitative trait locus enhances soybean 100-seed weight. *Molecular Plant*, 10, 670–684. https://doi.org/10.1016/j.molp.2017.03.006

Pitzschke, A., Djamei, A., Bitton, F. & Hirt, H. (2009) A major role of the MEKK1-MKK1/2-MPK4 pathway in ROS signalling. *Molecular Plant*, 2, 120–137. https://doi.org/10.1093/mp/ssn079

Pitzschke, A., Schikora, A. & Hirt, H. (2009) MAPK cascade signalling networks in plant defence. *Current Opinion in Plant Biology*, 12, 421–426. https://doi.org/10.1016/j.pbi.2009.06.008

Qiu, J.-L., Zhou, L.U., Yun, B.-W., Nielsen, H.B., Fiil, B.K., Petersen, K. et al. (2008) *Arabidopsis* mitogen-activated protein kinase kinases MKK1 and MKK2 have overlapping functions in defense signaling mediated by MEKK1, MPK4, and MKS1. *Plant Physiology*, 148, 212–222. https://doi.org/10.1104/pp.108.120006

Ren, Y., Armstrong, M., Qi, Y., McLellan, H., Zhong, C., Du, B. et al. (2019) *Phytophthora infestans* RXLR effectors target parallel steps in an immune signal transduction pathway. *Plant Physiology*, 180, 2227–2239. https://doi.org/10.1104/pp.18.00625

Rong, W., Feng, F., Zhou, J. & He, C. (2010) Effector-triggered innate immunity contributes *Arabidopsis* resistance to *Xanthomonas campestris*. *Molecular Plant Pathology*, 11, 783–793. https://doi.org/10.1111/j.1364-3703.2010.00642.x

Ryu, C.M., Anand, A., Kang, L. & Mysore, K.S. (2004) Agrodrench: A novel and effective agroinoculation method for virus-induced gene silencing in roots and diverse solanaceous species. *The Plant Journal*, 40, 322–331. https://doi.org/10.1111/j.1365-313X.2004.02211.x

Stulemeijer, I.J., Stratmann, J.W. & Joosten, M.H.A.J. (2007) Tomato mitogen-activated protein kinases LeMPK1, LeMPK2, and LeMPK3 are activated during the Cf-4/Avr4-induced hypersensitive response and have distinct phosphorylation specificities. *Plant Physiology*, 144, 1481–1494. https://doi.org/10.1104/pp.107.101063

Sun, K., Wolters, A.-M., Vossen, J.H., Rouwet, M.E., Loonen, A.E.H.M., Jacobsen, E. et al. (2016) Silencing of six susceptibility genes results in potato late blight resistance. *Transgenic Research*, 25, 731–742. https://doi.org/10.1007/s11248-016-9964-2

Teige, M., Scheikl, E., Eulgem, T., Dóczi, R., Ichimura, K., Shinozaki, K. et al. (2004) The MKK2 pathway mediates cold and salt stress signaling in *Arabidopsis*. *Molecular Cell*, 15, 141–152. https://doi.org/10.1016/j.molcel.2004.06.023

Virk, N., Liu, B.O., Zhang, H., Li, X., Zhang, Y., Li, D. et al. (2013) Tomato SlMPK4 is required for resistance against *Botrytis cinerea* and tolerance to drought stress. *Acta Physiologiae Plantarum*, 35, 1211–1221. https://doi.org/10.1007/s11738-012-1160-2

Vleeshouwers, V.G.A.A., Raffaele, S., Vossen, J.H., Champouret, N., Oliva, R., Segretin, M.E. et al. (2011) Understanding and exploiting late blight resistance in the age of effectors. *Annual Review of Phytopathology*, 49, 507–531. https://doi.org/10.1146/annurev-phyto-072910-095326

Wang, Y., Schuck, S., Wu, J., Yang, P., Döring, A.C., Zeier, J. et al. (2018) A MPK3/6-WRKY33-ALD1-pipecolic acid regulatory loop contributes to systemic acquired resistance. *The Plant Cell*, 30, 2480–2494. https://doi.org/10.1105/tpc.18.00547

Yamamizo, C., Kuchimura, K., Kobayashi, A., Katou, S., Kawakita, K., Jones, J.D.G. et al. (2006) Rewiring mitogen-activated protein kinase cascade by positive feedback confers potato blight resistance. *Plant Physiology*, 140, 681–692. https://doi.org/10.1104/pp.105.074906

Yuan, B., Shen, X., Li, X., Xu, C. & Wang, S. (2007) Mitogen-activated protein kinase OsMPK6 negatively regulates rice disease resistance to bacterial pathogens. *Planta*, 226, 953–960. https://doi.org/10.1007/s00425-007-0541-z

Zhang, T., Chhajed, S., Schneider, J.D., Feng, G., Song, W.Y. & Chen, S. (2019) Proteomic characterization of MPK4 signaling network and putative substrates. *Plant Molecular Biology*, 101, 325–339. https://doi.org/10.1007/s11103-019-00908-9

Zhang, M., Chiang, Y.H., Toruño, T.Y., Lee, D., Ma, M., Liang, X. et al. (2018) The MAP4 kinase SIK1 ensures robust extracellular ROS burst and antibacterial immunity in plants. *Cell Host & Microbe*, 24,379–391.e5. https://doi.org/10.1016/j.chom.2018.08.007

Zhang, T., Schneider, J.D., Lin, C., Geng, S., Ma, T., Lawrence, S.R. et al. (2019) MPK4 phosphorylation dynamics and interacting proteins in plant immunity. *Journal of Proteome Research*, 18, 826–840. https://doi.org/10.1021/acs.jproteome.8b00345

Zhang, Y. & Li, X. (2019) Salicylic acid: Biosynthesis, perception, and contributions to plant immunity. *Current Opinion in Plant Biology*, 50, 29–36. https://doi.org/10.1016/j.pbi.2019.02.004

Zhang, Z., Liu, Y., Huang, H., Gao, M., Wu, D., Kong, Q. et al. (2017) The NLR protein SUMM2 senses the disruption of an immune signaling MAP kinase cascade via CRCK3. *EMBO Reports*, 18, 292–302. https://doi.org/10.15252/embr.201642704

Zhang, Z., Wu, Y., Gao, M., Zhang, J., Kong, Q., Liu, Y. et al. (2012) Disruption of PAMP-induced MAP kinase cascade by a *Pseudomonas syringae* effector activates plant immunity mediated by the NB-LRR protein SUMM2. *Cell Host & Microbe*, 11, 253–263. https://doi.org/10.1016/j.chom.2012.01.015

Zhou, N., Tootle, T.L. & Glazebrook, J. (1999) Arabidopsis *PAD3*, a gene required for camalexin biosynthesis, encodes a putative cytochrome P450 monooxygenase. *The Plant Cell*, 11, 2419–2428. https://doi.org/10.1105/tpc.11.12.2419

Zhou, X.T., Jia, L.J., Wang, H.Y., Zhao, P., Wang, W.Y., Liu, N. et al. (2018) The potato transcription factor StbZIP61 regulates dynamic biosynthesis of salicylic acid in defense against *Phytophthora infestans* infection. *The Plant Journal*, 95, 1055–1068. https://doi.org/10.1111/tpj.14010

SUPPORTING INFORMATION

Additional supporting information may be found online in the Supporting Information section.